

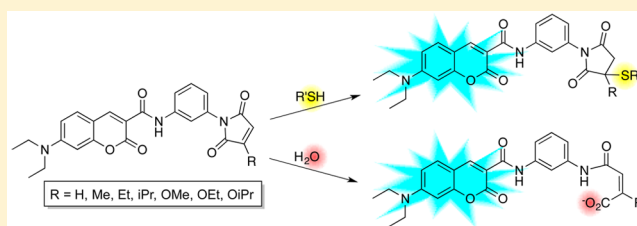
Ring Substituent Effects on the Thiol Addition and Hydrolysis Reactions of *N*-Arylmaleimides

Yingche Chen, Kelvin Tsao, Élise De Francesco, and Jeffrey W. Keillor*

Department of Chemistry and Biomolecular Sciences, University of Ottawa, 10 Marie-Curie, Ottawa, Ontario K1N 6N5, Canada

S Supporting Information

ABSTRACT: Maleimide groups are used extensively in bioconjugation reactions, but limited kinetic information is available regarding their thiol addition and hydrolysis reactions. We prepared a series of fluorogenic coumarin maleimide derivatives that differ by the substituent on their maleimide C=C bond. Fluorescence-based kinetic studies of the reaction with β -mercaptoethanol (BME) yielded the second-order rate constants (k_2), while pH–rate studies from pH 7 to 9 gave base-catalyzed hydrolysis rate constants (k_{OH}). Linear free-energy relationships were studied through the correlation of $\log k_2$ and $\log k_{\text{OH}}$ to both electronic (σ^+) and steric (E_s^{norm}) parameters of the C=C substituent. These correlations revealed the thiol addition reaction is primarily sensitive to the electronic effects, while steric effects dominate the hydrolysis reaction. These mechanistic studies provide the basis for the design of novel bioconjugation reactants or fluorogenic labeling agents.



INTRODUCTION

Bioorthogonal reactions are used extensively in chemical biology.^{1–3} In general, these are based on the chemoselective reactions between functional groups that are not prevalent in living systems. Some of the most commonly used bioorthogonal reactions include azide–alkyne cycloaddition,^{1,2} tetrazine ligation,¹ the Staudinger ligation,² and aldehyde/ketone condensations.² Other reactions have been developed for selectively targeting the functional groups of naturally occurring amino acids such as Lys, Tyr, and Cys.³

Maleimides are one of the most commonly used functional groups for performing bioconjugation reactions with thiols^{4–6} owing to the rapid Michael addition reaction⁷ that occurs in good yield under physiological conditions. Our group has exploited this thiol addition reaction in the development of enzyme inhibitors⁸ as well as site-specific fluorogenic protein labeling agents that comprise a phenyl ring bearing two maleimide groups that are meta to each other, positioning the reactive C=C bonds around 10 Å apart.^{9–13} The design of this dimaleimide moiety allows it to react efficiently with the two thiol groups of an α -helical peptide tag (“dC10 α ”) bearing two Cys residues separated by two turns of the α -helix, about 10 Å.¹¹ Although the rarity of this dicysteine motif confers substantial selectivity for the use of this labeling reaction in biological milieu,¹¹ the high intracellular concentration of glutathione (GSH), a thiol-containing tripeptide, posed a considerable challenge for the intracellular application of our method. Ultimately we were able to circumvent this problem by attenuating the reactivity of our dimaleimide labeling agents with adventitious thiols such as GSH through judicious maleimide ring substituent effects.¹³

Over the course of that work we were struck by the relatively limited detailed kinetic data available for maleimide reactions, which is especially surprising if one considers how frequently these reactions are used for bioconjugation. As discussed below, the hydrolysis of *N*-alkylmaleimides has been studied thoroughly,^{14,15} and their thiol addition reaction has also been examined.^{4,16} However, less attention has been given to the kinetics of the hydrolysis¹⁷ and thiol addition¹⁸ reactions of *N*-arylmaleimides. Furthermore, even fewer studies^{11,19} have examined the kinetic effects of substituents on the C=C double bond of the maleimide ring. Herein we present systematic kinetic studies of both the thiol addition and the hydrolysis reactions of *N*-arylmaleimides that reveal the maleimide ring substituent effects for each of these relevant reactions. The rate data and mechanistic conclusions of this study will be useful for the design of future probes and the optimization of protocols for their application to bioconjugation reactions.

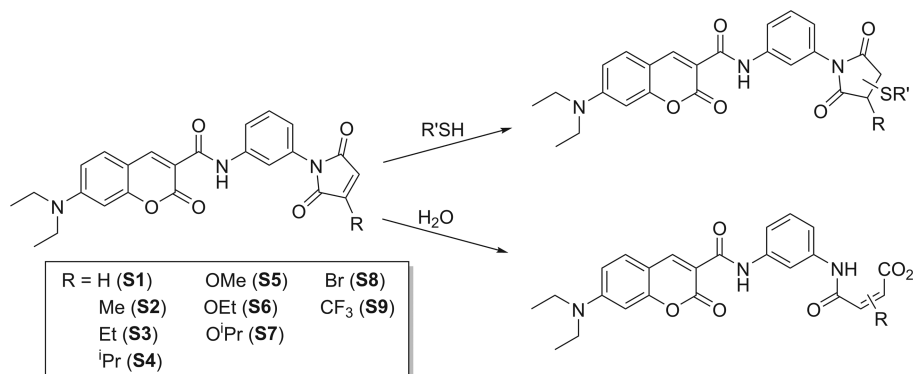
RESULTS AND DISCUSSION

Design and Synthesis. Historically, many kinetic studies of maleimide reactions have been conducted spectrophotometrically, following the decrease in absorbance at 302 nm upon the reaction of *N*-alkylmaleimides.^{4,14–16,20,21} However, the aromatic group of *N*-arylmaleimides makes the absorbance change at 302 nm more difficult to follow,¹⁸ which led us to explore the suitability of a fluorometric assay for kinetic studies of the reactions of this class of compounds. Kanaoka first reported that a maleimide group can suppress the latent

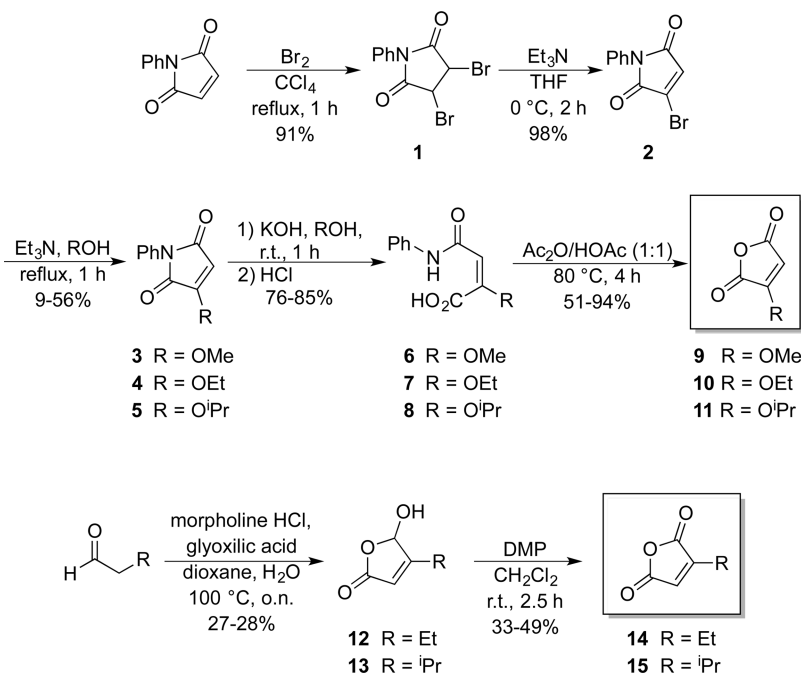
Received: September 10, 2015

Published: November 23, 2015

Scheme 1. Coumarin Maleimide Substrates S1–S8 and Their Hydrolysis and Thiol Addition Reactions Studied Herein



Scheme 2. Synthesis of Maleic Anhydride Intermediates



fluorescence of a pendant fluorophore,²² and many other fluorogenic maleimide derivatives have been prepared.^{23,24} Although originally it was suggested^{22,25} that the maleimide quenching mechanism may involve an $n \rightarrow \pi^*$ transition of the maleimide group, more recently we have shown^{10,12} that the quenching mechanism is based on photoinduced electron transfer (PeT) from the excited state of the fluorophore to the LUMO of the adjacent maleimide.²⁶ Coumarin was shown many years ago to be efficiently quenched by maleimides^{27–30} and has the advantage of being a particularly synthetically accessible fluorophore.^{31,32} Furthermore, the high quantum yield, photostability, and hydrophilicity of 7-diethylamino-3-carboxylcoumarin derivatives are qualities that are particularly well suited for long kinetic studies in aqueous solution.¹² This body of evidence inspired us to design a series of *N*-arylmaleimides bearing a 7-diethylaminocoumarin-3-ylcarboxamide moiety at the meta position, anticipating that the cyan fluorescence of the pendant coumarin should be restored¹³ upon reaction of the maleimide group (Scheme 1).

Our goal was therefore to prepare a diversified series of coumarin maleimides that differed only in the maleimide substituent (R, Scheme 1). Recently, amino-³³ and aryl-

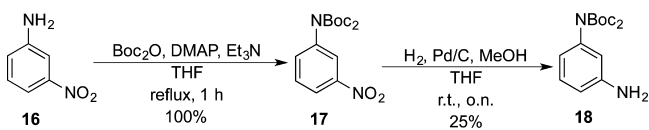
substituted³⁴ maleimides have been prepared by direct displacement or catalytic cross-coupling from bromomaleimides. In a similar fashion, we exploited the reactivity of bromomaleimides in a convergent synthetic approach where diversely substituted maleic anhydrides are added to a common primary amine at the end of the synthetic route. The synthesis of the key amine intermediate was also based on a convergent approach, involving the synthesis of the 7-diethylaminocoumarin 3-carboxylate fluorophore and the appropriately functionalized 1,3-diaminobenzene linker.

The required maleic anhydrides are either commercially available or were prepared as shown in Scheme 2. Specifically, *N*-phenylmaleimide was first subjected to dibromination prior to elimination of HBr to give the monobromo maleimide 2 in excellent yields. The bromide of 2 was displaced by ROH in low to moderate yield prior to ring-opening hydrolysis to give *N*-phenylmaleamic acids 6–8 in very good yields. Aniline was then eliminated from these maleamic acids in a ring-closing reaction that provided alkoxy-substituted derivatives 9–11 in moderate to excellent yields. Alternatively, alkyl-substituted anhydrides 14 and 15 were prepared by condensation of the initial aldehydes with glyoxylic acid, leading to lactones and

13 in moderate yields prior to oxidation to the desired anhydrides with Dess–Martin periodinane (DMP).

The diaminophenyl linker moiety was prepared asymmetrically in order to facilitate the protecting group strategy envisaged for the final conjugation procedure. To that end, *m*-nitroaniline was first protected with two Boc groups in quantitative yield. The nitro group was then reduced by palladium-catalyzed hydrogenation to give primary amine **18** (Scheme 3).

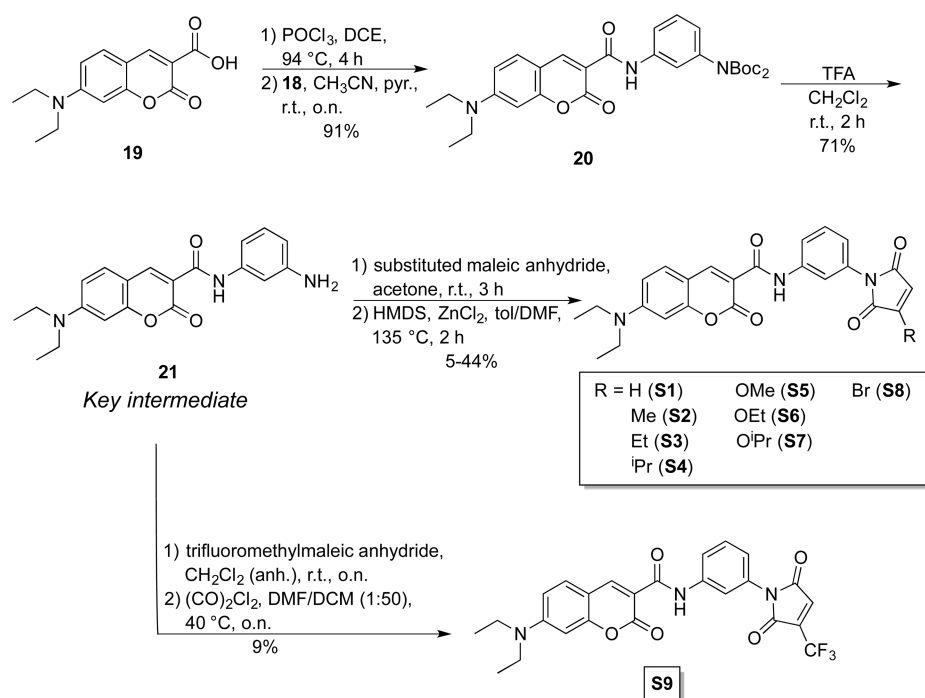
Scheme 3. Synthesis of Linker Intermediates



Coumarin fluorophore **19** was prepared as described previously,¹³ adapting a condensation reaction used to prepare similar coumarin analogues.³² Coupling with aniline linker **18** was accomplished by first converting acid **19** to its acid chloride. The resulting amide **20** was then deprotected quantitatively, giving key intermediate **21** as the final synthetic precursor (Scheme 4). The synthesis of **21** by an alternative route has also been reported very recently elsewhere.³⁵ Final substrates **S1–S9** were prepared by the reaction of **21** with the appropriate maleic anhydride. None of the synthetic steps were stringently optimized, since substrates **S1–S9** were prepared in sufficient yields to allow the kinetic studies central to this study.

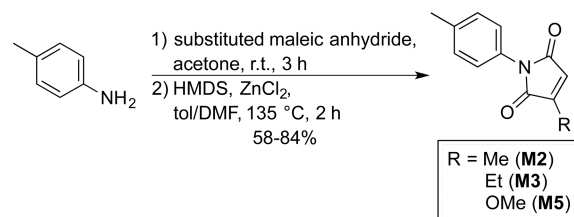
Product Studies. Given the dense functionalization of the coumarin maleimide substrates used in this work, product studies were first carried out to confirm their predicted reactivity. To this end, model compounds were designed with simpler structures in order to facilitate structural analysis by NMR. Although model compounds **M2** and **M3** are known,^{35–37} they were prepared for this study as shown in

Scheme 4. Synthesis of Final Coumarin Maleimide Substrates



Scheme 5 by reacting *p*-toluidine with the appropriate maleic anhydride to give model substrates **M2**, **M3**, and **M5**.

Scheme 5. Synthesis of Model Compounds for Product Studies



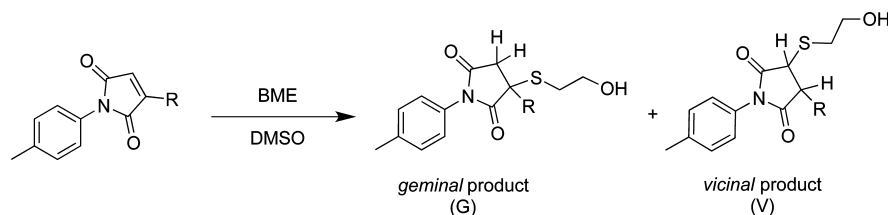
Thiol Addition. These model substrates were allowed to react with 1 equiv of β -mercaptoethanol (BME) in d_6 -DMSO in an NMR tube at room temperature overnight (see Experimental Section), and subsequent NMR analysis confirmed the formation of the expected thiol addition products. A singlet at 2.34 ppm, corresponding to the remote *p*-methyl substituent of the toluidine moiety of all three model compounds, remained unchanged in the formation of product and was therefore used as an integration standard. By this approach, the conversion of each reaction was determined, as shown in Table 1. The regioselectivity of each reaction was also

Table 1. Product Studies of Model Thiol Addition Reaction with BME (DMSO, 25 °C, overnight)

model compound	R	conversion (%)	regioselectivity (V:G)
M2	Me	92	58:42
M3	Et	80	84:16
M5	OMe	50	0:100

determined. For compound **M2**, the maleimide methyl substituent R appeared as a singlet at 1.64 ppm in the

Scheme 6. Regioselectivity of the Model Thiol Addition Reaction



Scheme 7. Resonance Model and Regioselectivity of M5 Thiol Addition

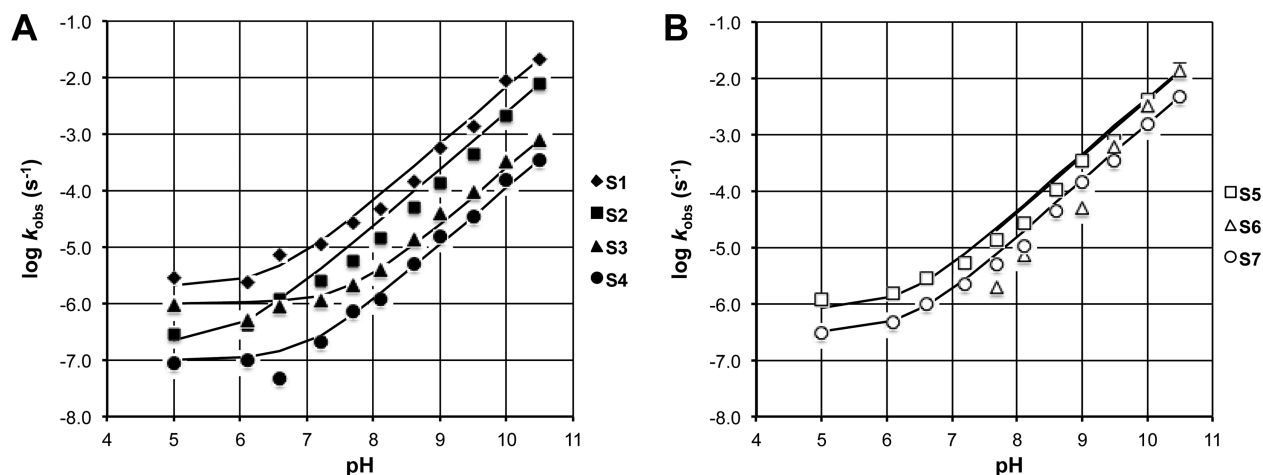
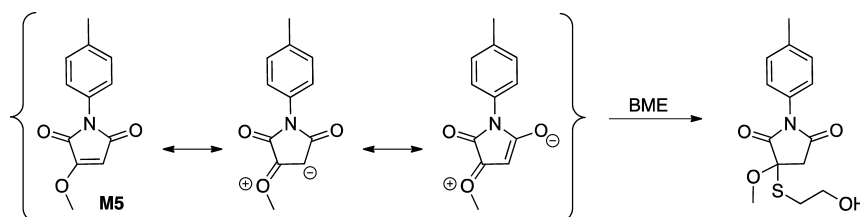


Figure 1. pH–rate profile for the hydrolysis of (A) substrates S1–S4 and (B) substrates S5–S7 (50 mM aqueous buffer, 5% DMSO, 22 °C). Solid lines are for fitted second-order rate constants, as described in the [Experimental Section](#).

“geminal” product (G) and as a doublet at 1.25 ppm in the “vicinal” product (V, see [Scheme 6](#)). For the ethyl derivative M3, the analysis was not quite as straightforward, but elucidation of coupling patterns in an additional COSY spectrum allowed the ethyl CH₂ group of G (1.8–2.0 ppm) to be distinguished from that of V (1.6–1.7 ppm) (see [Supporting Information](#)). Additional geminal coupling ($J = 18.4$ Hz) between the succinimide ring protons of G, appearing as doublets at 3.25 and 2.66 ppm, confirmed the integration of the assigned peaks. For the methyl-substituted maleimide, BME added preferentially to the less substituted carbon and even more so for the ethyl-substituted model compound, suggesting steric hindrance may account at least partially for the observed regioselectivity.

For the methoxy derivative M5, only one addition product was observed after 50% conversion. The presence of geminally coupled succinimide protons at 2.90 and 3.48 ppm confirmed it was the G regioisomer that was formed exclusively. This probably reflects the strong electron-donating character of the methoxy group through resonance with the maleimide double bond, increasing the electron density of the β -carbon ([Scheme 7](#)). This resonance delocalization is also reflected in the increased shielding of the maleimide proton of M5, whose

chemical shift is 6.01 ppm, compared to 6.77 and 6.75 ppm for the methyl and ethyl derivatives.

Finally, the effect of solvent on the regioselectivity of the thiol addition was examined by repeating the experiment with methyl model compound M2 in the presence of increasing amounts of D₂O. Interestingly, the V:G ratio shifted from 58:42 in 100% DMSO to 55:45 at 10% D₂O and 48:52 in 20% D₂O. This trend suggests that in the 95% water conditions of our kinetic studies (see below), the geminal addition product may be formed exclusively. However, we were unable to measure this directly, as we were unable to increase the concentration of D₂O above 20% while maintaining the concentrations necessary for NMR analysis due to the limited solubility of the model compound.

Hydrolysis. Model compounds M2, M3, and M5 were also subjected to hydrolysis and product analysis. As described in detail in the [Experimental Section](#), model compounds were hydrolyzed in the presence of 1% NaOH, and the resulting product mixture was extracted and analyzed by NMR. ¹H and ¹³C NMR indicated that only one hydrolysis product was formed for each of these reactions. Two-dimensional HMBC experiments showed a correlation between the carboxylate carbon of the maleamic acid product (see [Scheme 1](#)) and the

methyl protons of **M2** or the methylene protons of **M3**, indicating these two model compounds reacted exclusively through the carbonyl adjacent to the substituted carbon (see [Supporting Information](#)). After the reaction of compound **M5**, the methoxy proton in the sole hydrolysis product showed a correlation peak with the substituted alkene carbon, whose chemical shift (160.3 ppm) is consistent with an adjacent carboxylic acid rather than an adjacent anilide (expected 170 ppm). This indicates the reaction occurred with similar chemoselectivity.

Kinetic Studies. Hydrolysis. Although our primary interest is the fluorogenic thiol addition reaction of maleimide derivatives, it is also relevant to consider the stability of maleimides in aqueous solution, since maleamic acids do not show the same propensity for thiol addition reactions.³⁸ Previously it has been shown that *N*-phenylmaleimide undergoes hydrolysis 25 times more rapidly than *N*-ethylmaleimide (pH 7.0, 30 °C).¹⁷ However, at near neutral pH, *N*-arylmaleimides are still stable enough to be used for conjugation reactions, based on their much faster thiol addition reactions.^{11,18,24,39}

We sought to study the effect of maleimide ring substituents on their hydrolytic activity by measuring the rate constants of hydrolysis for our series of substrates from pH 5.0 to 10.5. We immediately observed that our most electrophilic substrate, **S9**, was highly prone to degradation in aqueous solution, leading to a multitude of products. This is consistent with McLeod's report¹⁹ that an *N*-aryl trifluoromethylmaleimide reacts completely with *N*-Ac-Cys-OH in <3 min in DMSO; however, we deemed that the kinetic investigation of **S9** in water would be highly impractical, so it was not studied further. In contrast, pseudo-first-order rate constants of hydrolysis (k_{obs}) were easily measured for substrates **S1–S7** (see [Experimental Section](#)), although the limited solubility of **S6** prevented its study below pH 7.7.

Three things are evident from the resulting plot of $\log k_{\text{obs}}$ vs pH ([Figure 1](#)). First, the pH–rate profile of each substrate appears to plateau from pH 5 to ~7. The pH independence over this range suggests the hydrolysis reaction may include a mechanistic pathway that involves the attack of neutral water on maleimide. Varying the concentration of buffer led to statistically insignificant variations in the measured rate constants, suggesting no buffer catalysis occurred. Second, the slope of the basic limb of the pH–rate profile can be fit to a slope of 1, indicating the reaction of 1 equiv of hydroxide above pH 7. Third, the second-order rate constants for reaction with hydroxide (k_{OH}) calculated for each substrate (see [Experimental Section](#)) differ significantly from one another, suggesting the hydrolysis reaction is sensitive to maleimide ring substituent effects (see below).

The second-order rate constants for hydroxide-catalyzed hydrolysis are shown in [Table 2](#). Very few rate constants have been reported for the hydrolysis of *N*-aryl maleimides. Salhany studied¹⁸ the hydrolysis of an unsubstituted maleimide bearing an eosin fluorophore on its ring nitrogen, showing a linear pH–rate profile from pH 7 to 10.2 (25 °C). Although no second-order rate constant was reported, half-lives corresponding to $\log k_{\text{obs}}$ values of -4.00 (pH 7.0) and -2.21 (pH 9.0) allow a rough comparison to the corresponding unsubstituted maleimide **S1** (see [Figure 1](#)) that indicate the latter is an order of magnitude less reactive. It is not surprising that the substituent on the maleimide nitrogen would influence its rate of hydrolysis; Kanaoka documented this effect thoroughly in a study of a series of six para-substituted *N*-phenylmaleimides.¹⁷

Table 2. Second-Order Rate Constants for Hydrolysis and BME Addition Reactions of *N*-Arylmaleimides

substrate	R	k_{OH} ($\text{M}^{-1} \text{s}^{-1}$)	k_2 ($\text{M}^{-1} \text{s}^{-1}$)	k_{OH}/k_2 ratio
S1	H	67 ± 17	8.9 ± 0.7	7.6
S2	Me	24 ± 4	4.4 ± 0.2	5.6
S3	Et	2.5 ± 0.5	2.2 ± 0.2	1.1
S4	ⁱ Pr	1.1 ± 0.3	1.3 ± 0.1	0.8
S5	OMe	45 ± 5	1.3 ± 0.1	40.5
S6	OEt	41 ± 7	N.D. ^a	
S7	O ⁱ Pr	15 ± 1	N.D. ^b	

^aNot determined: **S6** is not soluble in aqueous solution at pH 7.4, used for the thiol addition reactions. ^bNot determined: The hydrolysis of **S7** dominates at pH 7.4, used for the thiol addition reactions.

At pH 8.0, the reported half-lives correspond to $\log k_{\text{obs}}$ values from -3.46 (*p*-NMe₂) to -2.77 (*p*-NO₂) (30 °C), which are also 1–2 orders of magnitude greater than that of **S1**. The σ_{para} values of the substituents of Kanaoka's six substrates were used to provide a Hammett ρ value of +0.35 for the series, consistent with nucleophilic attack on the maleimide carbonyl being rate limiting.¹⁷

It is also instructive to compare our second-order rate constants with k_{OH} values measured for *N*-alkyl maleimides. Matsui reported¹⁵ k_{OH} values for a series of maleimides bearing H or alkyl groups on the maleimide nitrogen. These include *N*-ethylmaleimide (NEM), whose k_{OH} values were reported to be $34.7 \text{ M}^{-1} \text{ s}^{-1}$ at 20 °C and $46.8 \text{ M}^{-1} \text{ s}^{-1}$ at 30 °C, which are comparable to that of **S1** ([Table 2](#)). Furthermore, Matsui's pH–rate plot gives a $\log k_{\text{obs}}$ value of -5 for NEM at pH 7 (30 °C), which is also very similar to that measured for **S1** ([Figure 1](#)). From these comparisons it would appear that not all *N*-arylmaleimides are hydrolyzed more rapidly than all *N*-alkylmaleimides. Finally, by plotting the $\log k_{\text{OH}}$ values against the Taft polar parameter σ^* , the authors measured a ρ^* value of 0.55 (30 °C) for the series, consistent with attack by hydroxide being rate limiting for their *N*-alkylmaleimides.

Thiol Addition. Kinetic studies of the thiol addition reactions of substrates **S1–S7** were carried out at pH 7.4 and 37 °C in order to increase the relevance to in vivo labeling applications. Similarly, BME was used as a model thiol owing to its structural resemblance to biological thiols and its aqueous solubility. Kinetic reactions were performed under pseudo-first-order conditions using 25 μM substrate and 10–100 equiv of BME, allowing first-order rate constants to be measured from the monoexponential increase in fluorescence (see [Experimental Section](#)). Second-order rate constants (k_2) were then measured from the plots of k_{obs} vs [BME]. Under these conditions, **S6** was not sufficiently soluble to allow kinetic studies (see above), and substrate **S7** reacted so slowly that it was difficult to discern above background hydrolysis. However, for substrates **S1–S5**, the thiol addition reaction was typically >100-fold faster than background hydrolysis and easily measured.

The second-order rate constants (k_2) thus obtained for substrates **S1–S5** are shown in [Table 2](#). The unsubstituted maleimide **S1** had the highest rate constant for thiol addition and can be compared with a few values reported in the literature. For example, Bednar showed⁴ the reactivity of neutral BME with NEM is insignificant, but the thiolate of BME reacts with a rate constant of $1.8 \times 10^5 \text{ M}^{-1} \text{ s}^{-1}$ at 25 °C. The $\text{p}K_{\text{a}}$ of BME is 9.61;⁴⁰ correcting for the proportion of BME thiolate at pH 7.4 leads to a predicted rate constant for the reaction with NEM of $1.2 \times 10^3 \text{ M}^{-1} \text{ s}^{-1}$. This is lower than

the value of $9 \times 10^3 \text{ M}^{-1} \text{ s}^{-1}$ reported¹⁸ for the reaction of Cys with *N*-eosin-maleimide at pH 7.4 (25 °C) but very similar to the value of $1.1 \times 10^3 \text{ M}^{-1} \text{ s}^{-1}$ that we reported¹¹ previously for the reaction of GSH with a di-*N*-arylmaleimide fluorogen at pH 7.5 (20 °C). It is noteworthy that all of these rate constants are still 2 orders of magnitude higher than that measured for the reaction of BME with S1 ($8.9 \text{ M}^{-1} \text{ s}^{-1}$ from Table 2); however, the structural differences in the thiols and the maleimide *N*-substituent between all of these studies makes a direct comparison impossible.

It is also possible to note significant substituent effects for the thiol addition reaction in that the k_2 rate constants vary by nearly an order of magnitude from S1 down to S5. However, these substituent effects are less pronounced than those observed for hydrolysis, for which the k_{OH} values vary by nearly 2 orders of magnitude. Furthermore, it appears that a given substituent can have a different effect on the hydrolysis and thiol addition reaction. This is evident from the ratio of rate constants shown in Table 2. If the substituents had analogous effects on both reactions, one would expect the ratio of rate constants to be constant or to vary smoothly. However, while the methoxy substituent of S5 decreases its k_2 value relative to unsubstituted S1, it has very much less effect on the value of k_{OH} relative to S1. This suggests the mechanisms for the two reactions may show very different dependence on the substituents.

Linear Free Energy Relationships. Comparison of the first four entries of hydrolysis rate constants in Table 2 (S1–S4) reveals a significant effect of the steric bulk of the alkyl substituent on the hydrolytic reactivity. Further comparison of these values to those of the next three entries (S5–S7) suggests that the alkoxy substituents may promote hydrolysis relative to the alkyl substituents. However, it is difficult at first glance to separate the steric from the electronic effects of the substituents, implying that if a linear free energy relationship (LFER) exists for these rate data, it probably involves both steric and electronic parameters for the ring substituents. As mentioned above, different trends can be noted for the thiol addition rate constants, but these substituent effects probably involve both steric and electronic components also. From this it appears that the first step of more extended mechanistic analysis is the choice of appropriate substituent parameters.

In both hydrolysis and thiol addition reactions, maleimides react as electrophiles. Furthermore, the substituents of substrates S1–S9 are directly attached to the conjugated π system of the maleimide ring. These observations led us to propose that the Hammett σ^+ parameter may be an appropriate measure of the electronic effect of the substituents studied herein, including alkoxy substituents that can act as electron-donating groups through resonance delocalization.⁴¹ DFT calculations were performed on substrates S1–S9, providing density maps and energy levels for the LUMO of each molecule (see Table S1, Supporting Information). These energy levels correlate very well with the corresponding σ^+ values (see Figure S1, Supporting Information), as demonstrated recently for other systems,⁴² providing some confirmation that this substituent parameter is appropriate for measuring electronic effects.

However, plotting $\log k_{\text{OH}}$ and $\log k_2$ values against σ^+ values alone (Supporting Information, Figures S2 and S3) clearly illustrates the poor correlation between the measured rate constants and the isolated electronic substituent effects. Given the proximity of the maleimide ring substituent to the site of

nucleophilic attack, this is not surprising. In particular, the nucleophilic attack of thiolate on the substituted alkene carbon, giving rise to the G regioisomer discussed above, resembles the ester hydrolysis reaction chosen by Taft⁴³ for which he proposed the use of steric parameters. In Taft's model reaction, the steric effects of substituents on the C=O group of methyl esters were found to influence reaction rate in addition to their electronic effects, so it is reasonable to presume that this may also be true for thiolate attack on a substituted carbon of the C=C bond in the maleimide ring. Steric parameter values were therefore either taken directly from the literature⁴⁴ or calculated (see Supporting Information), then normalized to H, and subsequently used in the two-parameter fitting of $\log k_{\text{OH}}$ and $\log k_2$ values (see Table 3 and Experimental Section).

Table 3. Electronic (σ^+) and Steric Parameter (E_s^{norm}) Values Used Herein for the Substituents (R) of Substrates S1–S7

substrate	R	σ^+ ^a	E_s^{norm} ^b
S1	H	0.00	0.00
S2	Me	−0.31	−1.24
S3	Et	−0.29	−1.31
S4	ⁱ Pr	−0.28	−1.71
S5	OMe	−0.78	−0.25
S6	OEt	−0.81	−0.34
S7	O ⁱ Pr	−0.85	−0.82 ^c

^aTaken from ref 41. ^bTaken from ref 44. ^cCalculated from extrapolated values (see Supporting Information).

Two-parameter fitting of hydrolysis rate data of substrates S1–S7 gave an electronic reaction constant of $\rho = -0.1 \pm 0.5$ and a steric reaction constant of $\delta = 0.9 \pm 0.2$, leading to the plane shown in Figure 2 and the correlation of observed to predicted values shown in Figure S4 (Supporting Information). Although this correlation is significantly better than that

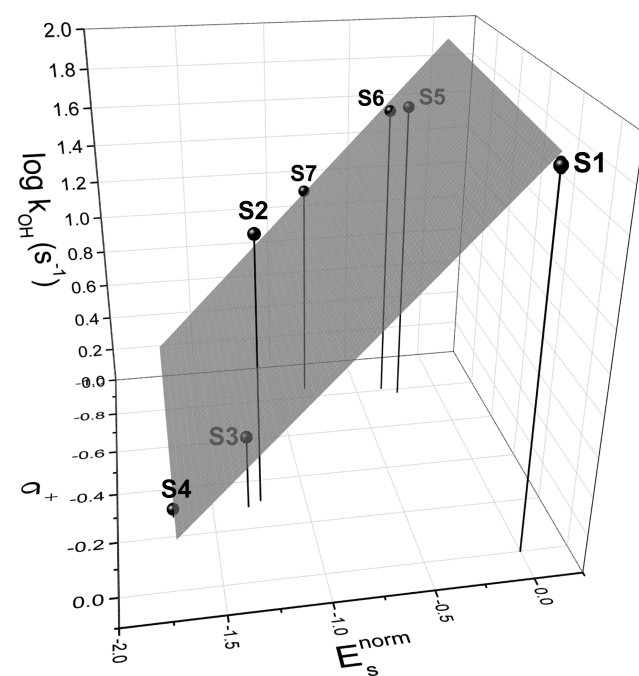


Figure 2. Plane fitted to the correlation of $\log k_{\text{OH}}$ values with both electronic (σ^+) and steric (E_s^{norm}) substituent parameters, yielding respective reaction constants of $\rho = -0.1 \pm 0.5$ and $\delta = 0.9 \pm 0.2$.

obtained for fitting with electronic parameters alone (not shown), it still only accounts for ~80% of the measured data points. Nevertheless, it is clear that the effect of ring substituent on the hydrolysis reaction is largely steric and minimally electronic. Assuming that hydroxide attack is rate limiting, as LFER studies of the hydrolysis of other maleimides have shown^{15,17} (see above), the significant δ value suggests the nucleophilic attack on at least one imide carbonyl may be hindered by the substituent, perhaps owing to the trajectory of the attack on the delocalized π^* system. Indeed, the results from our product studies indicate that the imide carbonyl that undergoes hydrolysis is the carbonyl *adjacent* to the substituted carbon, which may be the most sensitive to the steric bulk of that substituent. The fact that this carbonyl reacts preferentially may be due to the relief of steric strain between the carbonyl and the adjacent coplanar substituent upon formation of a tetrahedral intermediate during nucleophilic attack. The tetrahedral intermediate formed by attack on the carbonyl distal from the substituent would not benefit from this driving force due to ground state destabilization. Finally, the small ρ value measured for the hydrolysis reaction suggests that hydroxide may be a strong enough nucleophile to be insensitive to the electron effect of the substituent on the C=C bond.

For the rate data from the thiol addition reaction of substrates S1–S5, two-parameter fitting gave an electronic reaction constant of $\rho = 1.1 \pm 0.4$ and a steric reaction constant of $\delta = 0.2 \pm 0.4$. The plane defined by these fitted values is shown in Figure 3, and the correlation of predicted to measured

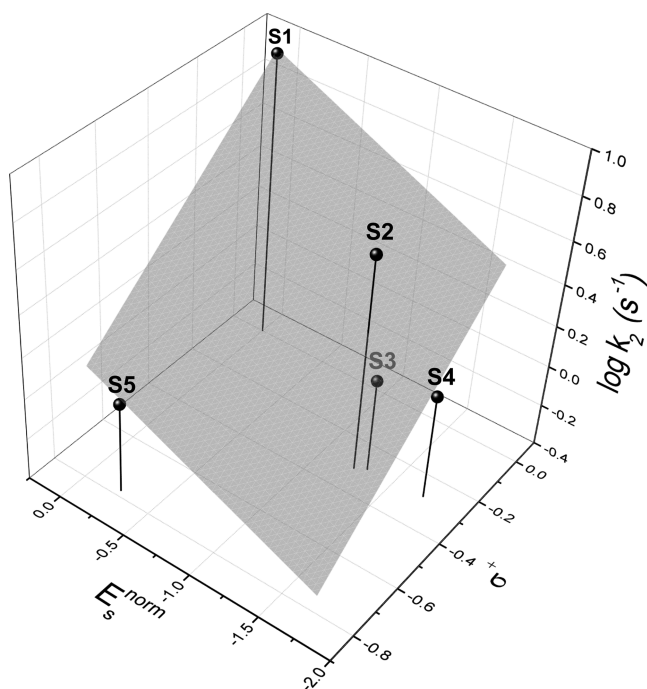


Figure 3. Plane fitted to the correlation of $\log k_2$ values with both electronic (σ^*) and steric (E_s^{norm}) substituent parameters, yielding respective reaction constants of $\rho = 1.1 \pm 0.4$ and $\delta = 0.2 \pm 0.2$.

rate constants is shown in Figure S5 (Supporting Information). The fitted values of these parameters suggest that the thiol addition reaction is unlike the hydrolysis reaction in that it is less sensitive to the steric effect of the substituent and more sensitive to its electronic effect. The smaller steric sensitivity of thiolate addition compared to hydrolysis may be due to the

greater polarizability of the larger S^- nucleophile compared to the smaller O^- nucleophile. The greater electronic sensitivity of thiolate addition can also be explained by the direct conjugation of the substituents with the reactive C=C bond as shown in Scheme 7.

However, the rough correlation shown in Figure 3 cautions against overinterpretation of the data. Moreover, as discussed above, the thiol addition reaction leads to the formation of two regioisomers. The rate constants for the formation of each of these regioisomers would presumably be affected differently by any given substituent, but our kinetic experiments, based on the appearance of total product, only inform us of the sum of the rate constants. Although knowledge of the ratio of these regioisomers would have allowed the correction of the observed second-order rate constants into relative rate constants for geminal and vicinal addition, we were unable to directly measure this ratio under the conditions of the kinetic experiments (5% DMSO) due to solubility issues (see above). This uncertainty with respect to regioselectivity underlines the intrinsic approximation in using only one pair of substituent parameters for substrates that may undergo two different (regioisomeric) reactions. However, taking into account the solvent-dependent regioselectivity that we were able to measure, we can conclude, at least qualitatively, that thiol addition is more sensitive to electronic than steric effects.

CONCLUSIONS

In summary, a series of ring-substituted maleimide derivatives was prepared, and the reactivity of these derivatives toward base-catalyzed hydrolysis and thiol addition was studied. Product studies indicate the hydrolysis reaction proceeds in a chemoselective manner, favoring the reaction of the carbonyl adjacent to the substituted carbon. The regioselectivity of the thiol addition reaction was found to depend upon the nature of the substituent. Two-parameter substituent effects indicate the hydrolysis rate constant is almost entirely dependent on the steric effect of the substituent, while the thiol addition reaction shows predominant dependence on the electronic effect of the substituent. These kinetic data and trends in reactivity should prove useful for the design of substituted maleimide derivatives for a variety of bioconjugation applications.

EXPERIMENTAL SECTION

General. All reagents and solvents for reactions were used as received unless otherwise stated. Dichloromethane, methanol, and tetrahydrofuran were dried by a solvent purification system. All reactions were performed under an inert atmosphere (e.g., N_2) in oven-dried glassware unless otherwise stated.

Reactions were monitored by thin layer chromatography (TLC) using silica gel precoated aluminum plates. Components were visualized by illumination with a short-wavelength ultraviolet light or long-wavelength visible light after which staining was performed with $KMnO_4$ solution followed by heating. Flash column chromatography was performed on silica gel (40–63 μm mesh) using ethyl acetate/*n*-hexane or acetonitrile/dichloromethane as eluting solvents.

Nuclear magnetic resonance (NMR) spectra were recorded in deuteriochloroform with tetramethylsilane (TMS) as internal reference at ambient temperature unless otherwise stated. Spectra were obtained at 400 or 500 MHz for ^1H and at 100.6 MHz for ^{13}C .

EI-MS spectra were recorded for both low-resolution and high-resolution mass spectra using a magnetic sector mass analyzer. ESI-MS spectra were recorded using a quadrupole-time-of-flight mass analyzer.

Ultraviolet absorption spectra and fluorescence spectroscopic studies were performed on a UV–vis microtiter plate reader.

Synthesis. Compounds **1–4**, **6**, **7**, **9**, and **10** were synthesized according to a literature procedure,⁴⁵ and isopropoxymaleic anhydride (**11**) was synthesized according to a similar procedure through intermediates **5** and **8**. Alkyl-substituted maleimides (**12–15**) were prepared by an aldol reaction, followed by oxidation of the alcohol to the ketone.⁴⁶

3-Isopropoxy-1-phenyl-1H-pyrrole-2,5-dione (5). To a suspension of 3-bromo-1-phenyl-1H-pyrrole-2,5-dione (**2**) (253 mg, 1 mmol) in isopropyl alcohol (4 mL) was added triethylamine (500 μ L, 3.6 mmol). The mixture formed was heated to reflux and stirred for 1 h. The reaction was cooled, and the solvents were removed by evaporation. The residue was purified by column chromatography to obtain compound **5** as yellow oil (20 mg, 9% yield). ¹H NMR (400 MHz, CDCl₃): δ (ppm) 7.45 (m, 2H), 7.31 (m, 3H), 5.45 (s, 1H), 4.51 (m, 1H), 1.46 (s, 3H), 1.44 (s, 3H). ¹³C NMR (100 MHz, CDCl₃): δ (ppm) 169.6, 158.9, 131.3, 129.0, 128.8, 127.7, 127.2, 126.4, 126.1. LRMS (EI) m/z (%): 231.1 (M⁺, 63%). HRMS (EI): calcd for C₁₃H₁₃NO₃ 231.0895. Found: 231.0888.

2-Isopropoxy-4-oxo-4-(phenylamino)but-2-enoic Acid (8). KOH (300 mg, 5.4 mmol) in H₂O (7.2 mL) was added to a solution of **5** (825 mg, 3.6 mL) in isopropyl alcohol (7.2 mL), and the mixture formed was stirred at ambient temperature for 1 h. After the starting material was totally consumed, the organic solvents were evaporated. The residue was acidified with concentrated HCl at 0 °C. The precipitate was filtered out and dried as crude product **8** (679 mg, 76% yield) and used in the following steps without further purification.

3-Isopropoxyfuran-2,5-dione (11). 2-Isopropoxy-4-oxo-4-(phenylamino)but-2-enoic acid (**8**) (679 mg, 2.73 mmol) was heated at 80 °C in a mixture of HOAc and Ac₂O (1:1, 18 mL) for 4 h. Ac₂O and HOAc were distilled off in vacuo, and the residue was purified by silica gel column chromatography to obtain **11** (400 mg, 94%) as a colorless oil. ¹H NMR (400 MHz, CDCl₃): δ (ppm) 5.62 (s, 1H), 4.51 (m, 1H), 1.46 (s, 3H), 1.43 (s, 3H). ¹³C NMR (100 MHz, CDCl₃): δ (ppm) 129.8, 128.7, 126.1, 97.9, 78.6, 27.0, 21.2. HRMS (EI): m/z calcd for C₇H₈O₄ ([M⁺]) 156.0423. Found: 156.0436.

4-Ethyl-5-hydroxyfuran-2(5H)-one (12).⁴⁷ Solid morpholine hydrochloride (3.4 g, 27.5 mmol) was added to a solution of glyoxylic acid monohydrate (2.3 g, 25 mmol) in 20 mL of dioxane. To this suspension was added dropwise 3 mL of H₂O, after which all of the solid material was dissolved. A solution of butyraldehyde (2.36 mL, 26.25 mmol) in 5 mL of dioxane was added via syringe, and the colorless solution was stirred at ambient temperature for 3 h and then heated to 100 °C and stirred overnight. The reaction mixture was evaporated and extracted 3 times with Et₂O, and the combined organic layers were then washed with saturated NaHCO₃ (aq) and brine, dried over MgSO₄, and concentrated. The residue was purified with column chromatography to obtain compound **12** as a colorless oil (850 mg, 27%). ¹H NMR (400 MHz, CDCl₃): δ (ppm) 6.00 (s, 1H), 5.83 (s, 1H), 4.85 (s, 1H), 2.44 (bs, 2H), 1.20 (t, J = 7.4 Hz, 3H). ¹³C NMR (100 MHz, CDCl₃): δ (ppm) 171.3, 116.8, 100.0, 99.0, 21.0, 10.9. LRMS (EI) m/z (%): 127.0 ([M - H]⁻, 13.4%). HRMS (EI): calcd for C₆H₈O₃ 127.0401. Found: 127.0377.

5-Hydroxy-4-isopropylfuran-2(5H)-one (13).⁴⁸ The above reaction was carried out with 3-methylbutanal, affording **13** as a colorless oil (983 mg, 28% yield). ¹H NMR (400 MHz, CDCl₃): δ (ppm) 6.07 (s, 1H), 5.79 (s, 1H), 2.72 (m, 1H), 1.19 (d, J = 6.8 Hz, 6H). ¹³C NMR (100 MHz, CDCl₃): δ (ppm) 171.3, 116.2, 98.3, 25.5, 22.4. HRMS (ESI): calcd for C₇H₁₀O₃Na ([MNa⁺]): 165.0528. Found: 165.0538.

3-Ethylfuran-2,5-dione (14).⁴⁹ Dess–Martin periodinane (3.40 g, 8.02 mmol) was suspended in anhydrous dichloromethane and stirred at room temperature for 10 min before a solution of compound **12** (856 mg, 6.68 mmol) in 20 mL of dichloromethane was added. The resulting mixture was stirred at room temperature for 2.5 h. The reaction mixture was then washed with saturated Na₂S₂O₃ (aq) and brine. The organic layer was dried over MgSO₄ and concentrated. The residue was purified by column chromatography as a colorless oil (413 mg, 49%). ¹H NMR (400 MHz, CDCl₃): δ (ppm) 6.60 (t, J = 2.0 Hz, 1H), 2.57 (qd, J = 7.4, 2.0 Hz, 2H), 1.28 (t, J = 7.4 Hz, 3H). ¹³C NMR (100 MHz, CDCl₃): δ (ppm) 165.7, 164.0, 155.1, 128.0, 19.6, 11.0.

LRMS (EI) m/z (%): 126.0 (M⁺, 14.6%). HRMS (EI): calcd for C₆H₆O₃ 126.0317. Found: 126.0311.

3-Isopropylfuran-2,5-dione (15).⁵⁰ The above reaction was carried out starting with 5-hydroxy-4-isopropylfuran-2(5H)-one (**13**), affording **15** as a colorless oil (324 mg, 33% yield). ¹H NMR (400 MHz, CDCl₃): δ (ppm) 6.44 (d, J = 1.6 Hz, 1H), 2.9 (m, 1H), 1.29 (s, 3H), 1.27 (s, 3H). ¹³C NMR (100 MHz, CDCl₃): δ (ppm) 165.2, 163.9, 127.0, 26.6, 23.5, 20.5. LRMS (EI) m/z (%): 140.0 (M⁺, 2.9%). HRMS (EI): calcd for C₇H₈O₃ 140.0473. Found: 140.0473.

tert-Butyl (3-Nitrophenyl)carbamate (17). To a solution of 3-nitroaniline (4.00 g, 29.0 mmol) in THF (40 mL) was added Boc₂O (19.0 g, 87.0 mmol), DMAP (26 mg, cat.), and Et₃N (10 mL, 73.0 mmol); this reaction mixture was heated to reflux for 3 h. The mixture was evaporated to remove solvents, and the residue was dissolved in Et₂O, washed with 1 N HCl (aq), NaHCO₃, and brine, dried over MgSO₄, and concentrated to obtain compound **17** as a white solid (4.99 g, 14.8 mmol) in 51% yield. ¹H NMR (400 MHz, CDCl₃): δ (ppm) 8.19 (m, 1H), 8.06 (t, J = 1.86 Hz, 1H), 7.54 (m, 2H), 1.45 (s, 18H). ¹³C NMR (100 MHz, CDCl₃): δ (ppm) 151.1, 148.4, 140.4, 134.4, 129.4, 123.5, 122.4, 83.8, 27.9. HRMS (ESI): m/z calcd for C₁₆H₂₂N₂O₆Na ([MNa⁺]): 361.1376. Found: 361.1360. Mp: 70.0 °C.

tert-Butyl (3-Aminophenyl)carbamate (18). *tert*-Butyl (3-nitrophenyl)carbamate (**17**) (2.50 g, 7.40 mmol) was dissolved in MeOH/THF (16 mL/24 mL), Pd/C (625 mg) was added to the solution, and the mixture was stirred under H₂ overnight. The Pd/C was removed by filtering through Celite, and the filtrate was evaporated to dryness. The residue was purified by column chromatography to yield compound **18** as a white solid (2.07 g, 6.72 mmol) in 91% yield. ¹H NMR (400 MHz, CDCl₃): δ (ppm) 7.11 (t, J = 7.94 Hz, 1H), 6.60 (ddd, J = 8.03, 2.25, 0.88 Hz, 1H), 6.54 (ddd, J = 7.84, 1.96, 0.90 Hz, 1H), 6.47 (t, J = 2.06 Hz, 1H), 3.67 (s, 2H), 1.43 (s, 18H). ¹³C NMR (100 MHz, CDCl₃): δ (ppm) 152.1, 146.9, 140.2, 129.4, 118.1, 114.7, 114.3, 82.5, 27.9. HRMS (ESI): m/z calcd for C₁₆H₂₂N₂O₄Na ([MNa⁺]): 331.1634. Found: 331.1645. Mp: 136.3 °C.

7-Diethylaminocoumarin-3-carboxylic acid (**19**) was synthesized according to a literature procedure.⁵¹

Preparation of Compound 20. Under nitrogen and anhydrous conditions, acid **19** (1.62 mg, 6.20 mmol) was dissolved in dichloroethane (60 mL). POCl₃ (2.9 mL, 31.0 mmol) was added, and the solution was brought to reflux for 4 h. Afterward, the solution was concentrated and the residue was dried under vacuum. Following this, the residue was dissolved in pyridine (60 mL) and aniline linker **18** (2.967 g, 9.30 mmol) was added. The mixture was stirred overnight at room temperature. The solvent was evaporated, and the crude solid was dissolved in DCM and washed with 0.1 M HCl and brine. The solution was dried with MgSO₄, which was removed through filtration, and the solution was concentrated to dryness. The crude product was purified by flash chromatography in 7:3 hexanes/ethyl acetate, and a yellow solid (1.23 g, 2.23 mmol) was obtained with a 36% yield. ¹H NMR (400 MHz, CDCl₃): δ (ppm) 10.92 (s, 1H), 8.78 (s, 1H), 7.65 (s, 1H), 7.64 (s, 1H), 7.46 (d, J = 9.01 Hz, 1H), 7.32 (t, J = 8.13 Hz, 1H), 6.90 (d, J = 8.23 Hz, 1H), 6.68 (dd, J = 9.01, 2.25 Hz, 1H), 6.53 (d, J = 2.06 Hz, 1H), 3.47 (q, J = 7.05 Hz, 4H), 1.43 (s, 18H), 1.26 (t, J = 7.10 Hz, 6H). ¹³C NMR (100 MHz, CDCl₃): δ (ppm) 163.1, 161.1, 157.8, 152.9, 151.8, 148.6, 139.9, 138.8, 131.3, 128.9, 123.6, 119.9, 119.1, 110.2, 110.1, 108.6, 96.6, 82.7, 45.2, 27.9, 12.4. HRMS (ESI): m/z calcd for C₃₀H₃₇N₃O₇Na ([MNa⁺]): 574.2529. Found: 574.2571. Mp: 170.7 °C.

Preparation of Key Intermediate 21, N-(3-Aminophenyl)-7-(diethylamino)-2-oxo-2H-chromene-3-carboxamide. Protected amine **20** (423 mg, 0.951 mmol) was dissolved in DCM (48 mL). TFA (10 mL) was added dropwise to the solution, which was stirred for 2 h at rt. The solvent was removed prior to dissolving the crude solid in a minimal amount of DCM and precipitating with acetonitrile. A yellow solid (324.8 mg, 0.924 mmol) was produced in 97% yield. Spectral data are essentially identical to those reported previously.³⁵ ¹H NMR (400 MHz, DMSO-*d*₆): δ (ppm) 10.73 (s, 1H), 8.71 (s, 1H), 7.70 (d, J = 9.1 Hz, 1H), 7.55 (s, 1H), 7.08–7.36 (m, 2H), 6.81 (dd, J = 2.4, 9.1 Hz, 1H), 6.73 (d, J = 7.5 Hz, 1H), 6.63 (d, J = 2.0 Hz, 1H),

3.47 (d, $J = 7.0$ Hz, 4H), 1.11 (t, $J = 7.0$ Hz, 6H). ^{13}C NMR (100 MHz, DMSO- d_6): δ (ppm) 162.72, 161.23, 157.89, 153.31, 148.67, 140.17, 139.65, 132.35, 130.39, 115.06, 114.46, 110.95, 110.58, 109.47, 108.38, 96.42, 44.90, 12.79. LRMS (ESI) m/z (%): 352.2740 (MH^+ , 34.1%). HRMS (ESI): m/z calcd for $\text{C}_{20}\text{H}_{21}\text{N}_3\text{O}_3\text{Na}$ ($[\text{MNa}^+]$): 374.1481. Found: 374.1497. Mp: 130.0 °C.

Preparation of Substrates S1–S8. Key intermediate **21** was dissolved in acetone (8 mL), and the corresponding maleic anhydride (1.5 equiv) was added to the solution. The mixture was stirred at 25 °C overnight. The solvents were evaporated under reduced pressure. The resulting residue was suspended in ether and vacuum filtered. The maleamic acid was collected as a dark brown solid and used in the next step of the reaction without further purification. ZnCl_2 (1.5 equiv) was dissolved in toluene–DMF (9:1 mL), and a dilute solution of HMDS (2.5 equiv) in toluene (2 mL) was added over 20 min. The resulting mixture was then heated to reflux for 3 h, after which the volatiles were evaporated under reduced pressure. The resulting residue was dissolved in EtOAc and washed with 0.1 M HCl and saturated Na_2CO_3 . The organic phase was dried with MgSO_4 . The drying agent was removed through filtration, and the solution was concentrated to dryness. The compound was purified using flash column chromatography in 6:4 hexanes/ethyl acetate to obtain S1–S8.

S1: Obtained 21.2 mg (49 μmol) of white solid in 35% yield. ^1H NMR (400 MHz, CDCl_3): δ (ppm) 10.96 (s, 1H), 8.75 (s, 1H), 7.85 (t, $J = 2$ Hz, 1H), 7.67 (m, 1H), 7.43 (m, 2H), 7.07 (m, 1H), 6.84 (s, 2H), 6.65 (dd, 1H, $J = 2.4, 9.0$ Hz), 6.51 (d, $J = 2.2$ Hz, 1H), 3.45 (q, $J = 7.1$ Hz, 4H), 1.25 (q, $J = 7.1$ Hz, 6H). ^{13}C NMR (100 MHz, CDCl_3): δ (ppm) 169.4, 163.1, 161.2, 157.8, 152.9, 148.7, 139.2, 134.2, 131.7, 131.4, 129.5, 121.7, 119.8, 118.1, 110.3, 109.9, 108.6, 96.7, 45.2, 14.1. LRMS (EI) m/z (%): 431.1434 (M^+ , 29.3%). HRMS (ESI): m/z calcd for $\text{C}_{24}\text{H}_{21}\text{N}_3\text{O}_5$ ($[\text{MNa}^+]$): 454.1379. Found: 454.1363. Mp: 167.8–168.0 °C.

S2: Obtained 9.6 mg of a yellow solid (22 μmol) in 7% yield; ^1H NMR (400 MHz, CDCl_3): δ (ppm) 10.95 (s, 1H), 8.76 (s, 1H), 7.82 (t, $J = 2.0$ Hz, 1H), 7.67 (m, 1H), 7.42 (m, 2H), 7.07 (m, 1H), 6.65 (dd, $J = 2.4, 8.9$ Hz, 1H), 6.54 (d, $J = 2.3$ Hz, 1H), 6.49 (q, $J = 1.7$ Hz, 1H), 3.45 (q, $J = 7.1$ Hz, 4H), 2.16 (d, $J = 1.8$ Hz, 3H), 1.23 (t, $J = 7.1$ Hz, 6H). ^{13}C NMR (100 MHz, CDCl_3): δ (ppm) 170.5, 169.4, 163.1, 161.2, 157.8, 152.9, 148.7, 145.8, 139.1, 132.1, 131.4, 129.4, 127.5, 121.6, 119.6, 118.0, 110.2, 110.0, 108.6, 96.6, 45.2, 12.4, 11.2. LRMS (EI) m/z (%): 445.1638 (M^+ , 13.2%). HRMS (ESI): m/z calcd for $\text{C}_{25}\text{H}_{23}\text{N}_3\text{O}_5$ ($[\text{M}^+]$) 445.1638. Found: 445.1638. Mp: 187.0–187.2 °C.

S3: Obtained 28.4 mg (61.8 μmol) of yellow solid in 44% yield. ^1H NMR (400 MHz, CDCl_3): δ (ppm) 10.94 (s, 1H), 8.74 (s, 1H), 7.82 (t, $J = 2.0$ Hz, 1H), 7.66 (m, 1H), 7.43 (m, 2H), 7.06 (dq, $J = 0.8, 7.9$ Hz, 1H), 6.65 (dd, $J = 8.9, 2.2$ Hz, 1H), 6.51 (d, $J = 2.0$ Hz, 1H), 6.41 (t, $J = 2.0$ Hz, 1H), 3.44 (q, $J = 7.1$ Hz, 4H), 2.53 (qd, $J = 1.9, 7.4$ Hz, 2H), 1.26 (t, $J = 7.3$ Hz, 3H), 1.22 (t, $J = 7.1$ Hz, 6H). ^{13}C NMR (100 MHz, CDCl_3): δ (ppm) 170.2, 169.6, 163.0, 161.2, 157.8, 152.8, 151.7, 148.6, 139.1, 132.1, 131.4, 129.4, 125.9, 121.6, 119.6, 118.0, 110.3, 110.1, 108.7, 96.8, 45.3, 19.1, 12.4, 11.3. LRMS (ESI) m/z (%): 482.0051 (MNa^+ , 100%). HRMS (ESI): m/z calcd for $\text{C}_{26}\text{H}_{25}\text{N}_3\text{O}_5\text{Na}$ ($[\text{MNa}^+]$): 482.1692. Found: 482.1678. Mp: 172.1–172.3 °C.

S4: Obtained 9.50 mg (19.3 μmol) of yellow solid in 14% yield. ^1H NMR (400 MHz, CDCl_3): δ (ppm) 10.94 (s, 1H), 8.76 (s, 1H), 7.83 (t, $J = 2.0$ Hz, 1H), 7.66 (m, 1H), 7.44 (d, $J = 9.0$ Hz, 1H), 7.40 (t, $J = 8.2$ Hz, 1H), 7.08 (m, 1H), 6.66 (dd, $J = 2.4, 9.0$ Hz, 1H), 6.52 (d, $J = 2.2$ Hz, 1H), 6.37 (d, $J = 1.6$ Hz, 1H), 3.45 (q, $J = 7.1$ Hz, 4H), 2.92 (sptd, $J = 1.5, 7.0$ Hz, 1H), 1.27 (d, $J = 6.9$ Hz, 6H), 1.23 (t, $J = 7.0$ Hz, 6H). ^{13}C NMR (100 MHz, CDCl_3): δ (ppm) 169.8, 163.1, 161.2, 157.8, 155.9, 152.8, 148.7, 139.1, 132.1, 131.4, 129.4, 128.8, 124.8, 121.7, 119.6, 118.1, 110.3, 110.1, 108.7, 96.8, 45.2, 25.9, 20.9, 12.4. LRMS (ESI) m/z (%): 496.1886 (MNa^+ , 100%). HRMS (EI): m/z calcd for $\text{C}_{27}\text{H}_{27}\text{N}_3\text{O}_5\text{Na}$ ($[\text{MNa}^+]$) 496.1848. Found: 496.1886. Mp: 154.1–154.3 °C.

S5: Obtained 3 mg (19 μmol) of white solid in 5% yield. ^1H NMR (400 MHz, CDCl_3): δ (ppm) 10.97 (s, 1H), 8.78 (s, 1H), 7.84 (s, 1H), 7.71 (d, $J = 8.0$ Hz, 1H), 7.44 (m, 2H), 7.09 (d, $J = 7.7$ Hz, 1H), 6.67 (d, $J = 8.7$ Hz, 1H), 6.53 (s, 1H), 5.57 (s, 1H), 4.01 (s, 3H), 3.47 (q, $J = 6.8$ Hz, 4H), 1.26 (t, $J = 6.7$ Hz, 6H). ^{13}C NMR (100 MHz, CDCl_3): δ (ppm) 168.8, 164.2, 163.1, 161.2, 160.8, 157.8, 152.9, 148.7, 139.1, 131.6, 131.4, 129.4, 121.7, 119.8, 118.1, 110.2, 110.0, 108.6, 96.7, 59.1, 45.2, 29.7, 12.4. LRMS (ESI) m/z (%): 462.0399 (MH^+ , 89.5%). HRMS (ESI): m/z calcd for $\text{C}_{25}\text{H}_{23}\text{N}_3\text{O}_6\text{Na}$ ($[\text{MNa}^+]$): 484.1485. Found: 484.1479. Mp: 182.8–183.0 °C.

S6: Obtained 29.5 mg (62.0 μmol) of a bright yellow solid in 44% yield. ^1H NMR (400 MHz, CDCl_3): δ (ppm) 10.94 (s, 1H), 8.74 (s, 1H), 7.79 (s, 1H), 7.69 (d, $J = 8.0$ Hz, 1H), 7.43 (m, 2H), 7.07 (d, $J = 7.9$ Hz, 1H), 6.64 (dd, $J = 2.2, 9.0$ Hz, 1H), 6.50 (d, $J = 2.0$ Hz, 1H), 5.50 (s, 1H), 4.19 (q, $J = 7.1$ Hz, 2H), 3.44 (q, $J = 7.1$ Hz, 4H), 1.51 (t, $J = 7.1$ Hz, 3H), 1.22 (t, $J = 7.1$ Hz, 6H). ^{13}C NMR (100 MHz, CDCl_3): δ (ppm) 169.1, 164.5, 163.1, 161.2, 159.8, 157.8, 152.9, 148.7, 139.1, 131.7, 131.4, 129.4, 121.8, 119.7, 118.2, 110.2, 110.0, 108.6, 96.7, 96.4, 68.6, 45.2, 13.9, 12.4. LRMS (ESI) m/z (%): 476.4018 (MH^+ , 7.2%). LRMS (ESI) m/z (%): 498.3858 (MNa^+ , 100%). HRMS (ESI): m/z calcd for $\text{C}_{26}\text{H}_{25}\text{N}_3\text{O}_6\text{Na}$ ($[\text{MNa}^+]$): 498.1641. Found: 498.1630. Mp: 238.5–238.7 °C.

S7: Obtained 16.7 mg (34.1 μmol) of a yellow solid in 24% yield. ^1H NMR (400 MHz, CDCl_3): δ (ppm) 10.93 (s, 1H), 8.75 (s, 1H), 7.79 (t, $J = 2.2$ Hz, 1H), 7.69 (d, $J = 8.1$ Hz, 1H), 7.44 (d, $J = 8.9$ Hz, 1H), 7.40 (t, $J = 8.1$ Hz, 1H), 7.07 (d, $J = 7.8$ Hz, 1H), 6.65 (dd, $J = 2.2, 9.0$ Hz, 1H), 6.51 (d, $J = 2.1$ Hz, 1H), 5.45 (s, 1H), 4.52 (spt, $J = 6.2$ Hz, 1H), 3.44 (q, $J = 7.1$ Hz, 4H), 1.46 (d, $J = 6.2$ Hz, 6H), 1.23 (t, $J = 7.1$ Hz, 6H). ^{13}C NMR (100 MHz, CDCl_3): δ (ppm) 169.4, 164.8, 163.0, 161.2, 158.9, 157.8, 152.9, 148.6, 139.1, 131.7, 131.4, 129.4, 121.8, 119.7, 118.2, 110.2, 110.0, 108.6, 96.6, 96.0, 45.2, 29.7, 21.2, 12.4. LRMS (ESI) m/z (%): 511.8859 (MNa^+ , 100%). HRMS (ESI): m/z calcd for $\text{C}_{27}\text{H}_{27}\text{N}_3\text{O}_6\text{Na}$ ($[\text{MNa}^+]$): 512.1797. Found: 512.1776. Mp: 197.9 °C.

S8: Obtained 15 mg (29 μmol) of a white solid in 21% yield; ^1H NMR (400 MHz, CDCl_3): δ (ppm) 10.98 (s, 1H), 8.75 (s, 1H), 7.87 (t, $J = 1.9$ Hz, 1H), 7.65 (d, $J = 8.2$ Hz, 1H), 7.40 (m, 2H), 7.09 (d, $J = 7.9$ Hz, 1H), 7.04 (s, 1H), 6.66 (dd, $J = 2.4, 9.0$ Hz, 1H), 6.52 (d, $J = 2.3$ Hz, 1H), 3.45 (q, $J = 7.1$ Hz, 4H), 1.27 (t, $J = 7.1$ Hz, 6H). ^{13}C NMR (100 MHz, CDCl_3): δ (ppm) 167.3, 164.1, 163.0, 161.3, 157.8, 152.9, 148.7, 139.3, 131.9, 131.8, 131.5, 131.4, 129.6, 121.6, 120.1, 118.1, 110.3, 109.9, 108.5, 96.7, 45.2, 12.4. LRMS (ESI) m/z (%): 532.0435 (MNa^+ , 100%). HRMS (ESI): m/z calcd for $\text{C}_{24}\text{H}_{20}\text{N}_3\text{O}_5\text{BrNa}$ ($[\text{MNa}^+]$): 532.0484. Found: 532.0467. Mp: 136.2–136.4 °C.

Preparation of S9. Under N_2 , trifluoromethylmaleic anhydride (1.5 eq, 0.450 mmol, 43.7 μL) in 10 mL of anhydrous DCM was added to a solution of **21** (100 mg, 0.300 mmol) dissolved in 5 mL of anhydrous DCM and stirred overnight. The solution was evaporated, and the residue was resuspended in 10 mL of Et_2O , after which the ether was removed and the residue dried. A round-bottom flask fitted with a condenser was purged and filled with N_2 before adding $(\text{CO})_2\text{Cl}_2$ (4.86 equiv, 127 μL , 1.46 mmol) and 0.3 mL of DMF through the condenser to limit water exposure; an additional 25 mL of DCM was then used to wash the condenser. The mixture was stirred at reflux overnight before solvent was removed by evaporation. The final product was purified from this mixture by flash chromatography using 6:4 hexanes/EtOAc as the eluent. A yellow solid (13.2 mg, 26.4 μmol) was obtained in 9.3% yield. ^1H NMR (400 MHz, CDCl_3): δ (ppm) 11.05 (s, 1H), 8.77 (s, 1H), 7.95 (t, $J = 1.8$ Hz, 1H), 7.67 (d, $J = 7.7$ Hz, 1H), 7.46 (m, 2H), 7.17 (q, $J = 1.8$ Hz, 1H), 7.08 (dd, $J = 7.9, 1.1$ Hz, 1H), 6.68 (dd, $J = 9.0, 2.4$ Hz, 1H), 6.54 (d, $J = 2.3$ Hz, 1H), 3.48 (q, $J = 7.2$ Hz, 4H), 1.26 (t, $J = 7.1$ Hz, 6H). ^{13}C NMR (100 MHz, CDCl_3): δ (ppm) 165.8, 163.1, 161.3, 157.9, 153.0, 148.8, 139.4, 133.4, 131.4, 130.8, 129.6, 121.6, 120.4, 118.1, 110.2, 109.7, 108.6, 96.6, 45.2, 12.4. LRMS (ESI) m/z (%): 522.0706 (MNa^+ , 100%). HRMS (ESI): m/z calcd for $\text{C}_{25}\text{H}_{20}\text{N}_3\text{O}_5\text{F}_3\text{Na}$ ($[\text{MNa}^+]$): 522.1240. Found: 522.1253. Mp: 173.2–173.3 °C.

Synthesis of Model Compounds M2, M3, and M5. *p*-Toluidine was dissolved in chloroform, and the corresponding maleic anhydride (1–1.5 equiv) was added to the solution. The mixture was stirred at 25 °C overnight. The solvents were then evaporated under reduced pressure. The resulting residue was suspended in ether and vacuum filtered. The maleamic acid intermediate was used in the next step of

the reaction without further purification. It was first dissolved in toluene–DMF (9:1 V/V) and ZnCl₂ (1.5 equiv), and then a dilute solution of HMDS (2.5 equiv) in toluene was added over 20 min. The resulting mixture was then heated to reflux for 3 h, after which the volatiles were evaporated under reduced pressure. The resulting residue was dissolved in EtOAc and washed with 0.1 M HCl and saturated Na₂CO₃. The organic phase was dried with MgSO₄. The drying agent was removed through filtration, and the solution was concentrated to dryness. The compound was purified using flash column chromatography in 8:2 hexanes/ethyl acetate to obtain the final model compounds.

M2: Obtained 1.69 g (8.4 mmol) of white solid in 84% yield. Spectral data are identical to those reported previously.⁵² ¹H NMR (400 MHz, CDCl₃): δ (ppm) 7.26 (d, *J* = 8.3 Hz, 2H), 7.20 (d, *J* = 8.3 Hz, 2H), 6.46 (t, *J* = 1.9 Hz, 1H), 2.38 (s, 3H), 2.17 (d, *J* = 1.8 Hz, 3H). ¹³C NMR (100 MHz, CDCl₃): δ (ppm) 170.8, 169.8, 145.8, 137.8, 129.7, 128.9, 127.4, 125.9, 21.2, 11.2. LRMS (EI) *m/z* (%): 201.1 (M⁺, 100). HRMS (EI): *m/z* calcd for C₁₂H₁₁NO₂ ([M⁺]) 201.0790. Found: 201.0785. Mp: 116.6–119.2 °C.

M3:³⁷ Obtained 282 mg (1.3 mmol) of white solid in 58% yield. ¹H NMR (400 MHz, CDCl₃): δ (ppm) 7.25 (d, *J* = 8.3 Hz, 2H), 7.20 (d, *J* = 8.5 Hz, 2H), 6.41 (t, *J* = 2.0 Hz, 1H), 2.53 (qd, *J* = 2.0, 7.4 Hz, 2H), 2.38 (s, 3H), 1.26 (t, *J* = 7.4 Hz, 3H). ¹³C NMR (100 MHz, CDCl₃): δ (ppm) 170.5, 169.9, 151.7, 137.7, 129.7, 129.0, 125.9, 125.8, 21.2, 19.1, 11.2. LRMS (EI) *m/z* (%): (M⁺, 100) 215.1. HRMS (EI): *m/z* calcd for C₁₃H₁₃NO₂ ([M⁺]) 215.0946. Found: 215.0974. Mp: 97.2–97.4 °C.

M5: Obtained 560 mg (2.6 mmol) of white solid in 66% yield. ¹H NMR (400 MHz, CDCl₃): δ (ppm) 7.25 (d, *J* = 8.7 Hz, 2H), 7.20 (d, *J* = 8.4 Hz, 2H), 5.54 (s, 1H), 3.97 (s, 3H), 2.37 (s, 3H). ¹³C NMR (100 MHz, CDCl₃): δ (ppm) 169.1, 164.5, 160.8, 137.9, 129.7, 128.4, 126.0, 96.4, 59.1, 21.2. LRMS (EI) *m/z* (%): (M⁺, 100) 217.0. HRMS (EI): *m/z* calcd for C₁₂H₁₁NO₃ ([M⁺]) 217.0739. Found: 217.0756. Mp: 184.3–184.4 °C.

Product Analyses. Three *N-p*-methylphenylmaleimides (**M2**, **M3**, and **M5**), synthesized as model compounds for substrates **S2**, **S3**, and **S5**, were subjected to thiol addition and hydrolysis reactions, and the products of those reactions were analyzed by NMR. For thiol addition, solutions were prepared of 150 μmol of each model compound in 1 mL of *d*₆-DMSO containing 1.0 equiv of BME (10.5 μL). A solution containing only the model compound served as a blank. After allowing each solution to react at room temperature overnight, 500 μL of the reaction mixture was transferred to an NMR tube and ¹H NMR spectra were recorded.

For the hydrolysis product studies, 10% NaOH was added to the model compounds dissolved in acetonitrile to make a final NaOH solution of 1% NaOH. The mixture was allowed to react for 3 h before removing the acetonitrile by rotary evaporation. The remaining solution was diluted with 10 mL of H₂O, and the respective maleamic acid was precipitated using 1 M HCl.

Hydrolyzed M2.³⁶ Obtained 51.8 mg (0.236 mmol) of a white solid in 48% yield. ¹H NMR³⁶ (400 MHz, DMSO-*d*₆): δ (ppm) 12.98 (bs, 1H), 10.10 (s, 1H), 7.50 (d, *J* = 8.43 Hz, 2H), 7.11 (d, *J* = 8.33 Hz, 2H), 6.10 (d, *J* = 1.47 Hz, 1H), 2.25 (s, 3H), 1.98 (d, *J* = 1.00 Hz, 3H). ¹³C NMR³⁶ (100 MHz, DMSO-*d*₆): δ (ppm) 170.0, 162.4, 142.4, 136.3, 132.4, 129.0, 123.2, 119.2, 20.5, 20.4. HRMS (EI): *m/z* calcd for C₁₂H₁₃NO₃ ([M⁺]) 219.08954. Found: 219.08679. Mp: 159.6–159.7 °C.

Hydrolyzed M3. Obtained 66.7 mg (0.286 mmol) of a yellow solid in 63% yield. ¹H NMR (400 MHz, DMSO-*d*₆): δ (ppm) 10.08 (s, 1H), 7.48 (d, *J* = 8.33 Hz, 2H), 7.10 (d, *J* = 8.23 Hz, 2H), 5.99 (s, 1H), 2.30 (q, *J* = 7.35 Hz, 2H), 2.23 (s, 3H), 1.05 (t, *J* = 7.40 Hz, 3H). ¹³C NMR (100 MHz, DMSO-*d*₆): δ (ppm) 170.7, 162.6, 149.1, 136.6, 132.8, 129.4, 120.8, 119.4, 27.3, 20.6, 11.9. HRMS (EI): *m/z* calcd for C₁₃H₁₅NO₃ ([M⁺]) 233.10519. Found: 233.10346. Mp: 132.9–133.0 °C.

Hydrolyzed M5. Obtained 101 mg (0.429 mmol) of a white solid in 93% yield. ¹H NMR (400 MHz, DMSO-*d*₆): δ (ppm) 10.04 (s, 1H), 7.45 (d, *J* = 8.43 Hz, 2H), 7.10 (d, *J* = 8.33 Hz, 2H), 5.54 (s, 1H), 3.68 (s, 3H), 2.23 (s, 3H). ¹³C NMR (100 MHz, DMSO-*d*₆): δ (ppm)

164.5, 163.5, 160.3, 136.7, 132.7, 129.4, 119.4, 96.7, 56.7, 20.6. HRMS (EI): *m/z* calcd for C₁₂H₁₃NO₄ ([M⁺]) 235.08446. Found: 235.08303. Mp: 179.8–179.9 °C.

Kinetic Studies. Kinetic experiments were carried out at either 22 (hydrolysis) or 37 °C (thiol addition) using either a Synergy H4 Hybrid Multi-Mode Microplate Reader with excitation and emission monochromators set at a 9 nm bandpass or an OLIS RSM 1000 stopped-flow fluorimeter. Buffered solutions containing different concentrations of BME were prepared in a 96-well plate or loaded into the stopped-flow filling syringe immediately before recording. Plate reader reactions were initiated by the addition of stock DMSO solutions of the coumarin *N*-arylmaleimide substrates (**S1–S7**), while stopped-flow reactions were initiated by mixing with a solution of substrate diluted in reaction buffer. Hydrolysis reactions were studied using 25 μM coumarin *N*-arylmaleimide substrate in final solutions containing 5% DMSO and buffers at pH 5.0 (50 mM acetate buffer), 6.1 (50 mM MES buffer), 6.6 (50 mM MES buffer), 7.2 (50 mM MOPS buffer), 7.7 (50 mM HEPES buffer), 8.1 (50 mM Tris buffer), 8.6 (100 mM Tris buffer), 9.0 (100 mM CHES buffer), 9.5 (50 mM CHES buffer), 10.0 (100 mM CAPS buffer), and 10.5 (50 mM CAPS buffer). Ionic strength was adjusted to 0.075 M by adding KCl. For thiol addition experiments the final reaction solution contained 25 μM coumarin *N*-arylmaleimide substrate and 0.250, 0.500, 0.750, 1.00, 1.25, 1.87, 2.50 mM BME in 50 mM HEPES buffer (pH 7.4) with 5% DMSO. Samples were excited at 440 nm, and fluorescence intensity was followed at 485 nm as a function of time. All curves of time-dependent fluorescence increase were followed over >5 half-lives and fitted by nonlinear regression to monoexponential eq 1

$$F_t = F_0 + F(1 - e^{-k_{\text{obs}}t}) \quad (1)$$

where F_t is the fluorescence intensity at time t , F_0 is the fluorescence intensity at time zero, F is the increase in fluorescence intensity, and k_{obs} is the measured pseudo-first-order rate constant.

For hydrolysis reactions, the second-order rate constant for hydroxide-catalyzed hydrolysis (k_{OH}) was calculated by plotting k_{obs} values against hydroxide concentration and fitting to eq 2

$$k_{\text{obs}} = k_w + k_{\text{OH}}[-\text{OH}] \quad (2)$$

where k_w is the rate constant for pH-independent reaction with water, observed below pH 7.

For thiol addition reactions, second-order rate constants (k_2) were calculated by plotting k_{obs} values against BME concentration and fitting to eq 3

$$k_{\text{obs}} = k_0 + k_2[\text{BME}] \quad (3)$$

where k_0 is the rate constant for the increase of fluorescence, extrapolated to zero BME. Under the conditions of the thiol addition reactions (pH 7.4) this was always observed to be negligible.

■ ASSOCIATED CONTENT

📄 Supporting Information

The Supporting Information is available free of charge on the ACS Publications website at DOI: 10.1021/acs.joc.5b02036.

NMR spectra for synthetic intermediates, final compounds tested herein, and product studies; DFT calculation coordinates and correlation analyses for LFERs (PDF)

■ AUTHOR INFORMATION

Corresponding Author

*E-mail: jkeillor@uottawa.ca

Notes

The authors declare no competing financial interest.

ACKNOWLEDGMENTS

The authors thank Dr. Glenn Facey of the departmental NMR Facility for his assistance with product analyses. This work was funded by the Natural Sciences and Engineering Research Council (NSERC, grant no. I2IPJ-452040) and the University of Ottawa (University Research Chair). K.T. thanks the Ontario Ministry of Training, Colleges, and Universities for an Ontario Graduate Scholarship (OGS).

REFERENCES

- (1) Ramil, C. P.; Lin, Q. *Chem. Commun. (Cambridge, U. K.)* **2013**, 49, 11007–11022.
- (2) Patterson, D. M.; Nazarova, L. A.; Prescher, J. A. *ACS Chem. Biol.* **2014**, *9*, 592–605.
- (3) Boutoureira, O.; Bernardes, G. J. L. *Chem. Rev.* **2015**, *115*, 2174–2195.
- (4) Bednar, R. A. *Biochemistry* **1990**, *29*, 3684–3690.
- (5) Kalia, J.; Raines, R. T. *Bioorg. Med. Chem. Lett.* **2007**, *17*, 6286–6289.
- (6) Fontaine, S. D.; Reid, R.; Robinson, L.; Ashley, G. W.; Santi, D. V. *Bioconjugate Chem.* **2015**, *26*, 145–152.
- (7) Michael, A. J. *Prakt. Chem.* **1886**, *35*, 349–356.
- (8) Halim, D.; Caron, K.; Keillor, J. W. *Bioorg. Med. Chem. Lett.* **2007**, *17*, 305–308.
- (9) Girouard, S.; Houle, M.-H.; Grandbois, A.; Keillor, J. W.; Michnick, S. W. *J. Am. Chem. Soc.* **2005**, *127*, 559–566.
- (10) Guy, J.; Caron, K.; Dufresne, S.; Michnick, S. W.; Skene, W. G.; Keillor, J. W. *J. Am. Chem. Soc.* **2007**, *129*, 11969–11977.
- (11) Guy, J.; Castonguay, R.; Campos-Reales Pineda, N. B.; Jacquier, V.; Caron, K.; Michnick, S. W.; Keillor, J. W. *Mol. Biosyst.* **2010**, *6*, 976–987.
- (12) Caron, K.; Lachapelle, V.; Keillor, J. W. *Org. Biomol. Chem.* **2011**, *9*, 185–197.
- (13) Chen, Y.; Clouthier, C. M.; Tsao, K.; Strmiskova, M.; Lachance, H.; Keillor, J. W. *Angew. Chem., Int. Ed.* **2014**, *53*, 13785–13788.
- (14) Heitz, J. R.; Anderson, C. D.; Anderson, B. M. *Arch. Biochem. Biophys.* **1968**, *127*, 627–636.
- (15) Matsui, S.; Aida, H. *J. Chem. Soc., Perkin Trans. 2* **1978**, 1277.
- (16) Lee, C. C.; Samuels, E. R. *Can. J. Chem.* **1964**, *42*, 168–170.
- (17) Machida, M.; Machida, M. I.; Kanaoka, Y. *Chem. Pharm. Bull.* **1977**, *25*, 2739–2743.
- (18) Schopfer, L. M.; Salhany, J. M. *Anal. Biochem.* **1998**, *257*, 139–148.
- (19) Ambrus, J. I.; Halliday, J. I.; Kanizaj, N.; Absalom, N.; Harpsøe, K.; Balle, T.; Chebib, M.; McLeod, M. D. *Chem. Commun. (Cambridge, U. K.)* **2012**, *48*, 6699–6701.
- (20) Gregory, J. D. *J. Am. Chem. Soc.* **1955**, *77*, 3922–3923.
- (21) Roberts, E.; Rouser, G. *Anal. Chem.* **1958**, *30*, 1291–1292.
- (22) Kanaoka, Y.; Sekine, T.; Machida, M.; Soma, Y.; Tanizawa, K.; Ban, Y. *Chem. Pharm. Bull.* **1964**, *12*, 127–134.
- (23) Kanaoka, Y. *Angew. Chem., Int. Ed. Engl.* **1977**, *16*, 137–147.
- (24) Corrie, J. E. T. *J. Chem. Soc., Perkin Trans. 1* **1994**, 2975–2982.
- (25) Kasha, M. *Discuss. Faraday Soc.* **1950**, *9*, 14–19.
- (26) Chen, Y.; Tsao, K.; Keillor, J. W. *Can. J. Chem.* **2015**, *93*, 389–398.
- (27) Machida, M.; Machida, M. I.; Sekine, T.; Kanaoka, Y. *Chem. Pharm. Bull.* **1977**, *25*, 1678–1684.
- (28) Sippel, T. O. *J. Histochem. Cytochem.* **1981**, *29*, 314–316.
- (29) Chaurasia, C. S.; Kauffman, J. M. *J. Heterocycl. Chem.* **1990**, *27*, 727–733.
- (30) Corrie, J. E. T. *J. Chem. Soc., Perkin Trans. 1* **1990**, 2151–2152.
- (31) Song, A.; Wang, X.; Lam, K. S. *Tetrahedron Lett.* **2003**, *44*, 1755–1758.
- (32) Orange, C.; Specht, A.; Puliti, D.; Sakr, E.; Furuta, T.; Winsor, B.; Goeldner, M. *Chem. Commun. (Cambridge, U. K.)* **2008**, 1217.
- (33) Mabire, A.; Robin, M. P.; Quan, W.; Willcock, H.; Stavros, V.; O'Reilly, R. K. *Chem. Commun. (Cambridge, U. K.)* **2015**, *51*, 9733–9736.
- (34) Awuah, E.; Capretta, A. *J. Org. Chem.* **2011**, *76*, 3122–3130.
- (35) Wang, M.; Wen, J.; Qin, Z.; Wang, H. *Dyes Pigm.* **2015**, *120*, 208–212.
- (36) Faturaci, Y.; Coşkun, N. *Turk. J. Chem.* **2012**, *36*, 749–758.
- (37) Botvinik, M. M.; Konovalov, I. M. *Zh. Obshch. Khim.* **1965**, *35*, 1127.
- (38) Ryan, C. P.; Smith, M. E. B.; Schumacher, F. F.; Grohmann, D.; Papaioannou, D.; Waksman, G.; Werner, F.; Baker, J. R.; Caddick, S. *Chem. Commun. (Cambridge, U. K.)* **2011**, *47*, 5452–5454.
- (39) Yang, J.-R.; Langmuir, M. E. *J. Heterocycl. Chem.* **1991**, *28*, 1177–1180.
- (40) Jencks, W. P.; Salvesen, K. *J. Am. Chem. Soc.* **1971**, *93*, 4433–4436.
- (41) Hansch, C.; Leo, A.; Taft, R. W. *Chem. Rev.* **1991**, *91*, 165–195.
- (42) Lincoln, R.; Greene, L. E.; Krumova, K.; Ding, Z.; Cosa, G. J. *Phys. Chem. A* **2014**, *118*, 10622–10630.
- (43) Taft, R. W. *J. Am. Chem. Soc.* **1952**, *74*, 3120–3128.
- (44) *Steric Effects in Organic Chemistry*; Taft, R. W., Jr.; Newman, M. S., Eds.; John Wiley & Sons, Inc.: New York, 1956.
- (45) Sahoo, M. K.; Mhaske, S. B.; Argade, N. P. *Synthesis* **2003**, *2003*, 346–349.
- (46) Parsons, W. H.; Du Bois, J. *J. Am. Chem. Soc.* **2013**, *135*, 10582–10585.
- (47) Laugraud, S.; Guingant, A.; D'Angelo, J. *J. Org. Chem.* **1987**, *52*, 4788–4790.
- (48) Bourguignon, J. J.; Wermuth, C. G. *J. Org. Chem.* **1981**, *46*, 4889–4894.
- (49) Miles, W. H.; Yan, M. *Tetrahedron Lett.* **2010**, *51*, 1710–1712.
- (50) Bernasconi, M.; Müller, M.-A.; Pfaltz, A. *Angew. Chem., Int. Ed.* **2014**, *53*, 5385–5388.
- (51) Ma, Y.; Luo, W.; Quinn, P. J.; Liu, Z.; Hider, R. C. *J. Med. Chem.* **2004**, *47*, 6349–6362.
- (52) Sortino, M.; Postigo, A.; Zacchino, S. *Molecules* **2013**, *18*, 5669–5683.